

SOLVING TIME-FRACTIONAL DIFFERENTIAL EQUATION VIA RATIONAL APPROXIMATION*

USTIM KHRISTENKO [†] AND BARBARA WOHLMUTH[†]

Abstract. Fractional differential equations (FDEs) describe subdiffusion behavior of dynamical systems. Its non-local structure requires to take into account the whole evolution history during the time integration, which then possibly causes additional memory use to store the history, growing in time. An alternative to a quadrature of the history integral is to approximate the fractional kernel with the sum of exponentials, which is equivalent to consider the FDE solution as a sum of solutions to a system of ODEs. One possibility to construct this system is to approximate the Laplace spectrum of the fractional kernel with a rational function. In this paper, we use the adaptive Antoulas–Anderson (AAA) algorithm for the rational approximation of the kernel spectrum which yields only a small number of real valued poles. We propose a numerical scheme based on this idea and study its stability and convergence properties. Moreover, we apply the algorithm to a time-fractional Cahn–Hilliard problem.

Key words. time-fractional differential equations, rational approximation, AAA algorithm

AMS subject classifications. 26A33, 34A08, 35R11, 41A20

1. Introduction. Fractional differential equations became a more and more popular research direction in the last decade, proposing new mathematical tools for describing complicated physical phenomena in case where the local differential models face their limitations. In particular, the time-fractional differential equations can be found in application such as, e.g., tumor growth models and in visco-elasticity. In the general case, the analytical solution of such problems is not available. Thus, the development and study of computational methods and algorithms for FDEs is of high interest and is the object of many research works. The numerical solution of a FDE is much more complicated and more computationally expensive than for the classical integer-order problem. In fact, the fractional ordinary differential equations (FODEs) are integral equations involving convolution with singular kernels. Thus, one of the related challenges is the non-local structure of the operators, which takes into account the whole evolution history during the time integration. This possibly causes additional memory use to store the history, which grows in time.

The most common strategy is directly based on the quadrature schemes for the convolution integral. The classical one is the so-called L1 scheme based on a finite difference formula [49, 33]. An important class constitutes the fractional linear multi-step methods (FLMM). Pioneering works in this direction has been done by Lubich [40, 41, 42]. The FLMM include methods of Adams–Moulton/Bashforth type [20, 21, 60, 62]. Though these methods are conceptually simple and have a high convergence order, they are shown to experience troubles for certain values of the fractional power [19]. Moreover, the quadrature-based approach is mostly affected by the curse of non-locality. Precisely, the integration of N time steps has algorithmic complexity of order $\mathcal{O}(N^2)$ and requires $\mathcal{O}(N)$ solutions to store. The non-locality problem can be tackled with various memory-saving techniques including short mem-

* Submitted December 23, 2024.

Funding: This work was funded by the German Research Foundation by grants WO671/11-1 and the European Union’s Horizon 2020 research and innovation programme under grant agreement No 800898.

[†]Lehrstuhl für Numerische Mathematik, Fakultät für Mathematik (M2), Technische Universität München, Garching bei München (khristen@ma.tum.de, wohlmuth@ma.tum.de)

ory principle [50, 14], logarithmic grid [29, 22] and parallel computations [18] for the history integral. Consequently, the complexity is possibly reduced to $\mathcal{O}(N \log N)$ with memory size $\mathcal{O}(\log N)$.

Another strategy for the numerical solution of FODEs is based on the approximation of the integral kernel. The crucial role in the approach plays an integral representation of the kernel. The first steps in this direction have been done in [43, 52, 39]. In the so-called kernel compression techniques, the kernel is approximated with a sum-of-exponentials [10, 45], leading to a family of ODEs, which can be usually solved in parallel. Therefore, this approach can be seen as a decomposition of the FODE solution into the sum of different modes, each governed by a corresponding local evolution law. This phenomenon clearly illustrates the nature of FODEs, where the computational complexity can be interpreted in terms of a hidden extra-dimension, which is also reflected in the methods for fractional partial differential equations (compare, e.g., with [12, 8, 11, 56, 31]). The advantage of this methodology is that the history term is approximated with a linear combination of a fixed number m of modes, and thus, no special treatment of the memory is needed with the constant additional storage of the size $\mathcal{O}(m)$ and the computational complexity $\mathcal{O}(Nm)$. In many works, the sum-of-exponentials is obtained using a quadrature for the integral representation of the kernel, see [37, 46, 32, 61, 2, 7]. An alternative approach for the approximation of the kernel consists in polynomial (multi-pole) interpolation of its spectrum [3]. Our approach belongs to this class. For the detailed overview of the existing numerical methods for FODE, we refer in particular to [6, 16, 23].

In this work, we propose a new approach based on the approximation of the Laplace spectrum of the convolution kernel with a rational function. We use the adaptive Antoulas–Anderson (AAA) algorithm [48], leading to a multi-pole approximation of the spectrum with real non-negative poles, which transforms to the sum-of-exponentials kernel with an additional singular term. In our numerical settings, we see that a small number of modes ($m \sim 20$) is sufficient to achieve excellent accuracy even in complex non-linear PDE test cases. Discretizing the obtained system of ODEs for the modes, we propose new numerical schemes of the Implicit Euler and Crank–Nicolson type. Though we do not discretize explicitly the local integration term, the local term coefficients in the numerical schemes, being defined by the rational approximation coefficients, naturally reproduce the fractional Adams–Moulton coefficients arising in linear multi-step methods.

The paper is structured as follows. In Section 2, we bring in the necessary definitions and formulations and provide some preliminary results. In Section 3, we discuss the rational approximation of the spectrum of the fractional kernel. In Section 4, we analyze the associated approximation error. In Section 5, we suggest numerical schemes based on the discretization of the modal ODE system and discuss their accuracy and stability. Finally, in Section 6, we illustrate the performance of the newly introduced schemes numerically. In particular, in Subsection 6.1, we consider a linear time-fractional heat equation in 1D with known analytical solution to show the convergence rate. In the second numerical example in Subsection 6.2, the proposed scheme is applied to a non-linear time-fractional Cahn–Hilliard equation in 2D.

2. Preliminaries. Let us first introduce some basic definitions of the fractional derivative and the fractional integral. For a more detailed introduction to the theory of fractional differential equations and fractional calculus, the reader is referred to [6,

4, 17, 36, 44, 50, 47, 51]. The Riemann–Liouville fractional integral is defined as

$$(2.1) \quad \mathcal{I}^\alpha u(t) = K_\alpha * u(t) = \int_0^t K_\alpha(t-s)u(s) \, ds,$$

where the kernel is defined by

$$K_\alpha(t) = t^{\alpha-1}/\Gamma(\alpha),$$

and $\Gamma(\alpha)$ is the gamma function. Then, the Riemann–Liouville fractional derivative is given by

$$\partial_t^\alpha u(t) = \partial_t [\mathcal{I}^{1-\alpha} u(t)].$$

If $u(t)$ is sufficiently smooth, then we have

$$\partial_t^\alpha [u(t) - u(0)] = \mathcal{I}^{1-\alpha} [\partial_t u(t)].$$

The right-hand side is the classical Caputo fractional derivative. The formulation on the left hand side, which expresses the Caputo fractional derivative in terms of Riemann–Liouville fractional derivative, has the advantage that it requires less regularity of $u(t)$ than the classical definition.

Let \mathcal{H} be a Hilbert space with inner product $\langle \cdot, \cdot \rangle$ and associated norm $\|\cdot\|_{\mathcal{H}}$. Let us consider the associated Bochner space $\mathcal{B} = L^2([0, T]; \mathcal{H})$ with the norm defined by $\|u\|_{\mathcal{B}}^2 = \int_0^T \|u(t)\|_{\mathcal{H}}^2 \, dt$. In the current work, we focus on the solution $u \in \mathcal{B}$ of the following non-linear fractional Cauchy problem:

$$(2.2) \quad \begin{aligned} \partial_t^\alpha u(t) &= F[u](t), \\ u(0) &= u_0, \end{aligned}$$

where $\alpha \in (0; 1]$, and $F : \mathcal{B} \rightarrow \hat{\mathcal{B}}$, with $\hat{\mathcal{B}} = L^2([0, T]; \mathcal{H}')$, is a continuous possibly non-linear operator. The solution of Equation (2.2) can be formally written in terms of (2.1) as

$$(2.3) \quad u(t) = u_0 + K_\alpha * F[u].$$

Let us denote by \mathfrak{L} the Laplace transform operator. Then, for any function $f \in \mathcal{B}$, we denote its Laplace transform by $\hat{f}(s) := \mathfrak{L}\{f\}(s) = \int_0^T f(t)e^{-st} \, dt$, $s \in \mathbb{C}$. In particular, the Laplace transform of (2.3) writes

$$\mathfrak{L}\{u - u_0\}(s) = s^{-\alpha} \mathfrak{L}\{F[u]\}(s).$$

We are interested in the construction of an approximation of $u(t)$ that we introduce through

$$(2.4) \quad \tilde{u}(t) = u_0 + \tilde{K}_\alpha * F[\tilde{u}],$$

where $\tilde{K}_\alpha(t)$ is an approximation of the kernel $K_\alpha(t)$.

3. Rational approximation of the kernel. We want to construct a kernel $\tilde{K}_\alpha(t)$ such that (2.4) yields a good approximation to the solution (2.3) of (2.2), which can be numerically found at a lower computational cost. Let us consider the

Laplace transforms of the kernels $K_\alpha(t)$ and $\tilde{K}_\alpha(t)$. We look for $\hat{\tilde{K}}_\alpha(z)$, $z \in \mathbb{C}$, in the form of a rational function, more precisely as a ratio of two polynomials. That is, we want to construct $\hat{\tilde{K}}_\alpha(z)$ as a rational approximation of $\hat{K}_\alpha(z) = z^{-\alpha}$. Since $\alpha \in (0, 1]$, we select the numerator and the denominator of $\hat{\tilde{K}}_\alpha(z)$ as polynomials of the same degree m . Under the assumption that the polynomials have only simple roots, the partial fractions decomposition of $\hat{\tilde{K}}_\alpha(z)$ writes:

$$(3.1) \quad \hat{\tilde{K}}_\alpha(z) = \sum_{k=1}^m \frac{c_k}{z + d_k} + c_\infty,$$

with $c_k \geq 0$, $d_k \geq 0$. Then, the kernel $\tilde{K}_\alpha(t)$ is given by a typical sum-of-exponentials and a singular term:

$$\tilde{K}_\alpha(t) = \sum_{k=1}^m c_k e^{-d_k t} + c_\infty \delta(t),$$

where $\delta(t)$ denotes the Dirac δ -distribution. Hence, the approximation $\tilde{u}(t)$, defined by (2.4), reads as

$$(3.2) \quad \tilde{u}(t) = u_0 + \sum_{k=1}^m u_k(t) + u_\infty(t),$$

where the modes $u_k(t)$ are given by

$$\begin{aligned} u_k(t) &= c_k \int_0^t e^{-d_k(t-\xi)} F[\tilde{u}](\xi) d\xi, \quad k = 1, \dots, m, \\ u_\infty(t) &= c_\infty F[\tilde{u}](t). \end{aligned}$$

That is, the modes $u_k(t)$, $k = 1, \dots, m$, satisfy the following ordinary differential equation:

$$(3.3) \quad \begin{aligned} \partial_t u_k(t) + d_k u_k(t) - c_k F[\tilde{u}] &= 0, \\ u_k(0) &= 0. \end{aligned}$$

Remark that the uni-modal ($m = 1$, $c_\infty = 0$) setting with $c_1 = 1$ and $d_1 = 0$ yields the trivial case $\alpha = 1$. On the other hand, the situation with only the "infinity" mode $c_\infty = 1$ ($m = 0$) corresponds to the case $\alpha = 0$.

Note that this expansion (3.2) is similar to the representations in [37, 59, 15], however we obtain the weights and exponents from the rational approximation of the kernel spectrum and not from the integral quadrature. The expansion coefficients c_k and d_k can be computed using various rational approximation algorithms, e.g., Padé approximant [5], Best Uniform Rational Approximation [53], barycentric rational interpolation [9], etc.. For more information on the rational interpolation methods, we refer to [55, 13]. In this work, we employ the adaptive Antoulas–Anderson (AAA) algorithm [48, Fig. 4.1], which in our test cases has demonstrated particular efficiency and robustness.

In order to compute the coefficients c_k and the poles $-d_k$ in the expansion (3.1), we implement the adaptive Antoulas–Anderson (AAA) algorithm [48, Fig. 4.1]. Let us consider the target function $f(z) = z^\alpha$ on the interval $[h, T]$. Without loss of

generality, we assume $T = 1$. Applying the AAA algorithm with the support points from $[h, T]$, using a logarithmic grid, we approximate the target function with a ratio of two polynomials of degree m :

$$P(z) = \sum_{k=0}^m p_k z^k \quad \text{and} \quad Q(z) = \sum_{k=0}^m q_k z^k.$$

Then, the rational function $r(z) = P(z^{-1})/Q(z^{-1}) = \sum_{k=0}^m p_k z^{m-k} / \sum_{k=0}^m q_k z^{m-k}$ approximates $f(z^{-1}) = z^{-\alpha}$ on the interval $[\frac{1}{T}, \frac{1}{h}]$. Hence, the partial fractions decomposition of $\hat{K}_\alpha(z) = r(z)$ yields the required multi-pole form (3.1).

Since the Laplace transform is a compact operator from $L^2([0, \infty])$ to $L^2([0, \infty])$, the problem of its inversion on the real line is, generally speaking, ill-posed [26]. Nevertheless, we observe that barycentric rational approximation on the real line leads to approximation on the vertical line in \mathbb{C} . However, the error on the vertical line is amplified with respect to the initial tolerance. In return, approximation on the real line provides real polynomial coefficients. Moreover, the coefficients $c_k \geq 0$ and $d_k \geq 0$ are non-negative.

To illustrate the accuracy, let us define the error of the kernel approximation as follows:

$$(3.4) \quad \mathcal{E}_{ra} := \left\| K_\alpha - \tilde{K}_\alpha^{Exp} \right\|_{L^1([h, T])} + \left| \int_0^h \left(K_\alpha(s) - \tilde{K}_\alpha^{Exp}(s) \right) ds - c_\infty \right|,$$

where we denote the sum-of-exponentials part of the kernel approximant by

$$\tilde{K}_\alpha^{Exp} := \sum_{k=1}^m c_k e^{-d_k t}.$$

In Figure 1 on the left, we show the convergence of this error with respect to the tolerance of the AAA algorithm for $T = 1$ and $h = 10^{-5}$. The integral in (3.4) is computed using *scipy* package [34]. Let us note that the above algorithm in our implementation faced its limitations with further decreasing both α and tolerance, when spurious poles appear.

In Figure 1 on the right, the number of modes m with the AAA-tolerance 10^{-12} is shown as function of the fractional power α for $T = 1$ and different h . We can remark a small number of modes in comparison with other multi-pole approximations, e.g., [3]. We can also observe that the number of modes decreases at the limits of the interval $(0, 1)$. Besides, for the value $\alpha = 1$, we obtain $m = 1$ with the single mode $c_1 = 1$ and $d_1 = 0$. For $\alpha = 0$, we have $m = 0$, when only the "infinity" mode $c_\infty = 1$ remains. Note that the coefficient c_∞ takes values between 0 and 1, where the extremities correspond respectively to $\alpha = 1$ and 0.

4. Error analysis. In this section, we estimate the error $\mathcal{E}_a(T) = \|u - \tilde{u}\|_B$ (Theorem 4.3 below). To this end, we will need the following auxiliary lemmas.

LEMMA 4.1. *Let $g \in L^1([0, T])$ and let $f(t) \in L^2([0, T])$ be uniformly Lipschitz continuous on $[0, T]$, i.e., there exists $C > 0$ such that for all $t_1, t_2 \in [0, T]$ it holds $|f(t_1) - f(t_2)| \leq C |t_1 - t_2|$. And let $c > 0$ be fixed. Then, for all $t \in [h, T]$, the*

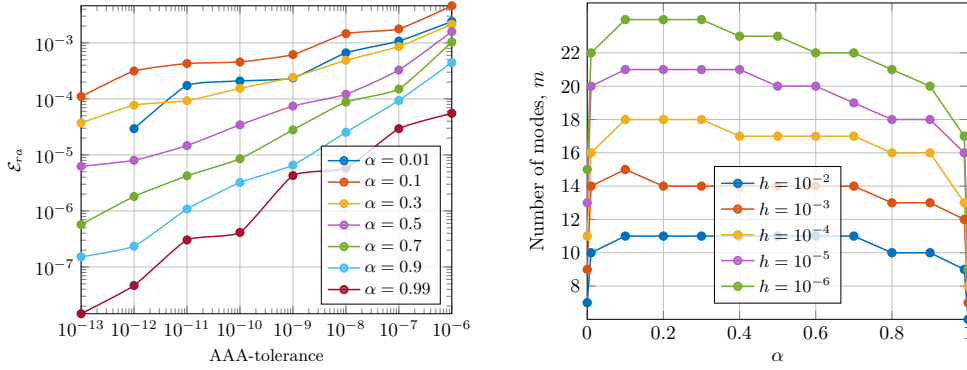


Fig. 1: **Left:** Dependence on the AAA algorithm tolerance of the rational approximation error (3.4) for $T = 1$ and $h = 10^{-5}$. **Right:** Dependence on α of the number of modes m with the AAA-tolerance 10^{-12} , $T = 1$ and different values of h .

following inequality holds

$$|g * f(t) - c f(t)| \leq C h \|g\|_{L^1([0, h])} + \left| \int_0^h g(s) ds - c \right| \cdot |f(t)| + g_{[h, T]} * f(t),$$

Proof. Adding $0 = c f(t) \int_0^h g(s) ds - c f(t) \int_0^h g(s) ds$, we can write

$$\int_{t-h}^t g(t-s) f(s) ds - c f(t) = \int_{t-h}^t g(t-s) [f(s) - f(t)] ds + \left[\int_0^h g(s) ds - c \right] f(t).$$

Note that by our continuity assumption, it holds for the first term that

$$\left| \int_{t-h}^t g(t-s) [f(s) - f(t)] ds \right| \leq C h \|g\|_{L^1([0, h])}.$$

Hence follows the statement. \square

LEMMA 4.2 (Grönwall inequality). *Let $v \in \mathcal{B}$, $\varepsilon \in L^2([0, T])$ and a constant $C > 0$ such that*

$$(4.1) \quad \|v(t)\|_{\mathcal{H}} \leq |\varepsilon(t)| + C (K_{\alpha} * \|v\|_{\mathcal{H}})(t).$$

Then,

$$(4.2) \quad \|v\|_{\mathcal{B}} \leq \|\varepsilon\|_{L^2([0, T])} \cdot E_{\alpha, 1}[C T^{\alpha}],$$

where $E_{\alpha, \beta}[x]$ denotes Mittag-Leffler function [35]:

$$(4.3) \quad E_{\alpha, \beta}[x] = \sum_{k=0}^{\infty} \frac{x^k}{\Gamma(\alpha k + \beta)}.$$

Proof. According to [58, Theorem 1], it follows from (4.1)

$$\|v(t)\|_{\mathcal{H}} \leq |\varepsilon(t)| + \int_0^t \sum_{k=1}^{\infty} \frac{C^k (t-s)^{\alpha k-1}}{\Gamma(\alpha k)} |\varepsilon(s)| ds.$$

Hence, computing the L^2 -norm on $[0, T]$ and applying Young's convolution inequality to the last term, we obtain

$$\|v\|_{\mathcal{B}} \leq \|\varepsilon\|_{L^2([0, T])} \cdot \left(1 + \sum_{k=1}^{\infty} \frac{C^k T^{\alpha k}}{\Gamma(\alpha k + 1)} \right),$$

which corresponds to (4.2). \square

THEOREM 4.3. *Let $F : \mathcal{B} \rightarrow \hat{\mathcal{B}}$ be a uniformly Lipschitz continuous operator, i.e., there exist $C_1 > 0$ and $C_2 > 0$ such that for any $v_1, v_2 \in \mathcal{B}$, $v_3 \in \mathcal{H}$ and $t \in [0, T]$,*

$$(4.4) \quad |\langle F[v_1](t) - F[v_2](t), v_3 \rangle_{\mathcal{H}', \mathcal{H}}| \leq C_1 \|v_1(t) - v_2(t)\|_{\mathcal{H}} \cdot \|v_3\|_{\mathcal{H}}.$$

and for $h > 0$,

$$|\langle F[v_1](t+h) - F[v_1](t), v_3 \rangle_{\mathcal{H}', \mathcal{H}}| \leq C_2 h \|v_3\|_{\mathcal{H}}.$$

And let

$$u(t) = u_0 + K_{\alpha} * F[u], \quad \tilde{u}(t) = u_0 + \tilde{K}_{\alpha} * F[\tilde{u}],$$

such that for $h > 0$, there exists $C_{\alpha} > 0$ that $\|K_{\alpha} - \tilde{K}_{\alpha}^{Exp}\|_{L^1([0, h])} \leq C_{\alpha} h^{\alpha}$ and

$$(4.5) \quad \left| \int_0^h (K_{\alpha}(s) - \tilde{K}_{\alpha}^{Exp}(s)) ds - c_{\infty} \right| + \|K_{\alpha} - \tilde{K}_{\alpha}^{Exp}\|_{L^1([h, T])} \leq C_{\alpha} h^{1+\alpha}.$$

Then, the following error estimate holds:

$$(4.6) \quad \|u - \tilde{u}\|_{\mathcal{B}} \leq h^{1+\alpha} \cdot 2C_{\alpha} E_{\alpha,1}[C_1 T^{\alpha}] \cdot (C_2 + \|\partial_t^{\alpha} u\|_{\hat{\mathcal{B}}}).$$

Proof. Let us introduce $w(t) = u_0 + K_{\alpha} * F[\tilde{u}](t)$. Then, adding $0 = w - w$, we find for the norm

$$(4.7) \quad \|u - \tilde{u}\|_{\mathcal{H}}^2 \leq |\langle u - w, u - \tilde{u} \rangle_{\mathcal{H}}| + |\langle w - \tilde{u}, u - \tilde{u} \rangle_{\mathcal{H}}|.$$

We denote by $g = K_{\alpha} - \tilde{K}_{\alpha}^{Exp}$ the difference of the kernels, and by $g_{[a,b]}$ a function which coincides with g on $[a, b]$ and vanishes elsewhere. Note that we can write formally

$$(K_{\alpha} - \tilde{K}_{\alpha}) * F[u] = \int_{t-h}^t g(t-s) F[u](s) ds - c_{\infty} F[u](t) + g_{[h, T]} * F[u].$$

Then, by Lemma 4.1, the first term in (4.7) can be bounded as

$$(4.8) \quad |\langle u - w, u - \tilde{u} \rangle_{\mathcal{H}}| = \left| \langle (K_{\alpha} - \tilde{K}_{\alpha}) * F[\tilde{u}], u - \tilde{u} \rangle_{\mathcal{H}} \right| \leq \varepsilon(t) \cdot \|u - \tilde{u}\|_{\mathcal{H}},$$

where the error $\varepsilon(t)$ is defined as

$$(4.9) \quad \varepsilon(t) := C_2 h \|g\|_{L^1([0,h])} + \left| \int_0^h g(s) ds - c_\infty \right| \cdot \|F[\tilde{u}]\|_{\mathcal{H}'} + |g_{[h,T]}| * \|F[\tilde{u}]\|_{\mathcal{H}'}.$$

By the continuity assumption (4.4), the following upper bound holds for the second term in (4.7):

$$(4.10) \quad |\langle w - \tilde{u}, u - \tilde{u} \rangle_{\mathcal{H}}| = |\langle K_\alpha * (F[u] - F[\tilde{u}]), u - \tilde{u} \rangle_{\mathcal{H}}| \leq C_1 (K_\alpha * \|u - \tilde{u}\|_{\mathcal{H}}) \cdot \|u - \tilde{u}\|_{\mathcal{H}}.$$

Substituting (4.8) and (4.10) to (4.7), we obtain

$$\|u - \tilde{u}\|_{\mathcal{H}} \leq \varepsilon(t) + C_1 (K_\alpha * \|u - \tilde{u}\|_{\mathcal{H}}).$$

Hence, by Lemma 4.2, we have

$$(4.11) \quad \|u - \tilde{u}\|_{\mathcal{B}} \leq \|\varepsilon\|_{L^2([0,T])} \cdot E_{\alpha,1}[C_1 T^\alpha].$$

Using Young's convolution inequality and (4.5), we obtain from (4.9):

$$(4.12) \quad \|\varepsilon\|_{L^2([0,T])} \leq C_2 h \|g\|_{L^1([0,h])} + \left[\left| \int_0^h g(s) ds - c_\infty \right| + \|g\|_{L^1([h,T])} \right] \cdot \|F[\tilde{u}]\|_{\mathcal{B}} \leq C_\alpha h^{1+\alpha} (C_2 + \|F[\tilde{u}]\|_{\mathcal{B}}).$$

Moreover, by the continuity (4.4), it holds that

$$(4.13) \quad \|F[\tilde{u}]\|_{\mathcal{B}} \leq \|F[u]\|_{\mathcal{B}} + \|F[u] - F[\tilde{u}]\|_{\mathcal{B}} \leq \|\partial_t^\alpha u\|_{\mathcal{B}} + C_1 \|u - \tilde{u}\|_{\mathcal{B}}.$$

Thus, under condition that $C_1 C_\alpha h^{1+\alpha} \leq 1/2$, combining (4.11), (4.12) and (4.13), we eventually obtain (4.6). \square

5. Numerical schemes. Let us denote by \tilde{u}_h the numerical approximation of \tilde{u} , defined by (3.2), and by $u_{h,k}$ the approximations of the modes u_k , $k = 1, \dots, m$, in (3.3). The discretized solution of the system of equations (3.3) can be numerically computed with any known numerical scheme. The simplest case of the so-called θ -scheme, including Euler and Crank-Nicolson time-integration, is introduced in the following proposition.

PROPOSITION 5.1. *Applying a standard θ -scheme to the modal system (3.3), it straightforwardly yields the following scheme for (3.2):*

$$(5.1) \quad \tilde{u}_h^{n+1} - \beta^1 F[\tilde{u}_h^{n+1}] = \beta^2 F[\tilde{u}_h^n] + u_0 + \sum_{k=1}^m \gamma_k u_{h,k}^n,$$

where the discrete modes $u_{h,k}^n$, $k = 1, \dots, m$, are updated by

$$(5.2) \quad u_{h,k}^{n+1} = \gamma_k u_{h,k}^n + \beta_k^1 F[\tilde{u}_h^{n+1}] + \beta_k^2 F[\tilde{u}_h^n], \quad u_{h,k}^0 = 0,$$

with coefficients

$$(5.3) \quad \beta_k^1 = \frac{c_k \theta h}{1 + \theta d_k h}, \quad \beta_k^2 = \frac{c_k (1 - \theta) h}{1 + \theta d_k h}, \quad \gamma_k = \frac{1 - (1 - \theta) d_k h}{1 + \theta d_k h},$$

$$\beta^1 = \sum_{k=1}^m \beta_k^1 + c_\infty, \quad \beta^2 = \sum_{k=1}^m \beta_k^2.$$

Remark 5.2. The coefficient β^1 corresponds to the expansion (3.1) and thus approximates $(\theta h)^\alpha$. Moreover, we have $\beta^1 = (\theta h)^\alpha$ if $z = \theta h$ is a support point in the AAA algorithm.

Remark 5.3. When $\alpha = 1$, there is only one mode $c_1 = 1$, $d_1 = 0$, therefore, the above scheme reduces to the classical integer-order θ -scheme.

Let us note that the proposed scheme does not require the solution of a large coupled system of equations, but consists in alternating updates of the full solution \tilde{u}_h , Eq. (5.1), and updates of the modes $u_{h,k}$, Eq. (5.2). A graphical illustration of the algorithm is suggested in Figure 2. The modes updates (5.3) are completely decoupled and can be computed in parallel. Besides, they are linear. A non-linear equation of the original size has to be solved only once per time-step in (5.1), using any preferred non-linear solver (e.g., Newton-Raphson or Fixed-point). In particular, in the PDE case, when F involves a spacial differential operator, the PDE system is solved only in (5.1). Moreover, for the updates (5.3), one does not even have to solve a mass matrix system. Indeed, instead of computing the modes $u_{h,k}^n$, $k = 1, \dots, m$, themselves, one can proceed with numerical integration computing only $M u_{h,k}^n$, where M stands for the formal mass matrix. And no explicit computation of the modes is necessary for computing the full solution \tilde{u}_h^n .

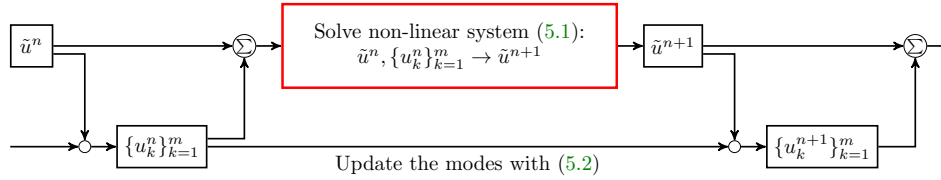


Fig. 2: Scheme of the n -th time iteration, representing the system (5.1)-(5.2). Both the integral approximation \tilde{u}^n and the family of modes $\{u_k^n\}_{k=0}^m$ have to be updated in each time step. However, each step requires only one non-linear system of the original size to solve.

The proposed θ -scheme is simple, however, it does not guarantee unconditional stability for an arbitrary operator F . In particular, unconditionally stable schemes are usually based on the splitting of the operator [27, 28]. So, let us consider F in the form $F[v] = F_-[v] + F_+[v]$, where the monotonous operators F_- and F_+ corresponds to the decreasing and strictly increasing parts of F , respectively. That is, for all $v_1, v_2 \in \mathcal{B}$, it holds

$$\langle F_-[v_1] - F_-[v_2], v_1 - v_2 \rangle_{\mathcal{H}} \leq 0, \quad \langle F_+[v_1] - F_+[v_2], v_1 - v_2 \rangle_{\mathcal{H}} > 0.$$

In addition, we rewrite the continuity condition with some $C_F > 0$ in the form

$$\|F_-[v_1] - F_-[v_2]\|_{\mathcal{H}'} + \|F_+[v_1] - F_+[v_2]\|_{\mathcal{H}'} \leq C_F \|v_1 - v_2\|_{\mathcal{H}}.$$

In the following lemmas, we propose numerical schemes for such F and estimate the associated discretization error $\epsilon_h^n := \|\tilde{u}(t^n) - \tilde{u}_h^n\|_{\mathcal{H}}$. We also introduce the modal discretization errors $\epsilon_{h,k}^n := \|u_k(t^n) - u_{h,k}^n\|_{\mathcal{H}}$.

Let us also briefly remark that the solution of a FDE usually exhibits a weak singularity at the initial time. So, the approximation error near the origin has to be

treated in a special way, see, e.g., [41, 62]. For the following error estimates, we focus on the evolution far enough from the singularity and thus assume the initial state to be smooth enough to ignore this effect.

LEMMA 5.4 (Implicit Euler). *Let \tilde{u}_h^n be defined by the following time-stepping scheme:*

$$(5.4) \quad \tilde{u}_h^{n+1} - \beta F_-[\tilde{u}_h^{n+1}] = \beta F_+[\tilde{u}_h^n] + u_0 + \sum_{k=1}^m \gamma_k u_{h,k}^n,$$

where the discrete modes $u_{h,k}^n$, $k = 1, \dots, m$, are updated by

$$(5.5) \quad u_{h,k}^{n+1} = \gamma_k u_{h,k}^n + \beta_k F[\tilde{u}_h^{n+1}], \quad u_{h,k}^0 = 0,$$

with coefficients given by

$$\gamma_k = \frac{1}{1 + d_k h}, \quad \beta_k = \frac{c_k h}{1 + d_k h}, \quad \beta = \sum_{k=1}^m \beta_k + c_\infty.$$

Then, \tilde{u}_h^n approximates $\tilde{u}(t)$, provided the discretization error of order h :

$$\epsilon_h^n = \|\tilde{u}(t^n) - \tilde{u}_h^n\|_{\mathcal{H}} \leq \mathcal{O}(mh) \cdot e^{C_F[(t^n)^\alpha + \varepsilon_{ra}]},$$

where $\varepsilon_{ra} := \max_{s \in [\frac{1}{T}, \frac{1}{h}]} |\hat{K}(s) - \hat{\tilde{K}}(s)|$ stands for the rational approximation error.

Proof. Taylor expansion of $u_k(t^n)$ at the point t^{n+1} , with the first derivative given by (3.3), yields

$$u_k(t^{n+1}) = u_k(t^n) - h \underbrace{(d_k u_k(t^{n+1}) - c_k F[\tilde{u}](t^{n+1}))}_{\partial_t u_k(t^{n+1})} + \mathcal{O}(h^2).$$

Hence, we express $u_k(t^{n+1})$:

$$(5.6) \quad u_k(t^{n+1}) = \gamma_k u_k(t^n) + \beta_k F[\tilde{u}](t^{n+1}) + \gamma_k \mathcal{O}(h^2).$$

Summing up the modes, u_0 and u_∞ , we obtain

$$\tilde{u}(t^{n+1}) - \beta F[\tilde{u}](t^{n+1}) = u_0 + \sum_{k=1}^m \gamma_k u_k(t^n) + \mathcal{O}(mh^2).$$

Note that $\beta = \mathcal{O}(h^\alpha)$. Then, using Taylor expansion of $F_+[\tilde{u}](t^{n+1})$ at the point t^n , we can write

$$(5.7) \quad \tilde{u}(t^{n+1}) - \beta F_-[\tilde{u}](t^{n+1}) = \beta F_+[\tilde{u}](t^n) + u_0 + \sum_{k=1}^m \gamma_k u_k(t^n) + \mathcal{O}(mh^2 + h^{1+\alpha}).$$

Recall that F is Lipschitz continuous and F_- monotonously decreases, which implies

$$(5.8) \quad \begin{aligned} & |\langle F[\tilde{u}](t^n) - F[\tilde{u}_h], \tilde{u}(t^n) - \tilde{u}_h^n \rangle_{\mathcal{H}}| \leq C_F |\epsilon_h^n|^2, \\ & \langle F_-[\tilde{u}](t^n) - F_-[\tilde{u}_h], \tilde{u}(t^n) - \tilde{u}_h^n \rangle_{\mathcal{H}} \leq 0. \end{aligned}$$

Thus, subtracting (5.4) and (5.5) from (5.7) and (5.6), respectively, we obtain

$$(5.9) \quad \epsilon_h^{n+1} \leq \beta C_F \epsilon_h^n + \sum_{k=1}^m \gamma_k \epsilon_{h,k}^n + \mathcal{O}(mh(h + h^\alpha/m)),$$

and

$$(5.10) \quad \epsilon_{h,k}^{n+1} \leq \gamma_k \epsilon_{h,k}^n + \beta_k C_F \epsilon_h^{n+1} + \mathcal{O}(h^2), \quad \epsilon_{h,k}^0 = 0.$$

Recursive substitution in (5.10) yields to

$$\epsilon_{h,k}^n \leq \beta_k C_F \sum_{j=1}^n \gamma_k^{n-j} \epsilon_h^j + \mathcal{O}(h).$$

And substituting this to (5.9), we end up with

$$\epsilon_h^{n+1} \leq \beta C_F \epsilon_h^n + C_F \sum_{k=1}^m \sum_{j=1}^n \beta_k \gamma_k^{n+1-j} \epsilon_h^j + \mathcal{O}(mh), \quad \epsilon_h^0 = 0.$$

Hence, the discrete Grönwall inequality completes the proof:

$$\epsilon_h^n \leq \mathcal{O}(mh) \cdot e^{C_F [\sum_{k=1}^m \sum_{j=0}^{n-1} \beta_k \gamma_k^j + c_\infty]} \leq \mathcal{O}(mh) \cdot e^{C_F [(t^n)^\alpha + \varepsilon_{ra}]},$$

where we used the following bound for the exponent:

$$\sum_{j=0}^{n-1} \beta_k \gamma_k^j = \beta_k \frac{1 - \gamma_k^n}{1 - \gamma_k} = c_k \frac{1 - \gamma_k^n}{d_k} \leq \frac{c_k}{d_k} \left(1 - \frac{1}{1 + nd_k h} \right) \leq \frac{c_k n h}{1 + d_k n h}.$$

□

Remark 5.5. Remark that the case $\theta = 1/2$ in Proposition 5.1, the Crank-Nicolson scheme (CN), is known to be not A-stable. Indeed, we have $-1 \leq \gamma_k \leq 1$ in (5.3) with $\theta = 1/2$, moreover, γ_k approaches -1 for large enough d_k , giving rise to a stiff problem. Thus, the higher modes produce undesired oscillation of the solution. Since $\max d_k$ grows when α decays, the oscillations become more dominant the smaller α is. An example can be found in the next section (Figure 4). This observation motivates us to introduce in the following lemma a modified scheme which expresses more stability but preserves the order.

LEMMA 5.6 (Modified Crank-Nicolson). *Let \tilde{u}_h^n be defined by the following time-stepping scheme:*

$$(5.11) \quad \tilde{u}_h^{n+1} - \beta F_-[\tilde{u}_h^{n+1}] = \beta F_+[\tilde{u}_h^n] + u_0 + \sum_{k=1}^m \gamma_k u_{h,k}^n,$$

where the discrete modes u_k^n , $k = 1, \dots, m$, are updated by

$$(5.12) \quad u_{h,k}^{n+1} = \gamma_k u_{h,k}^n + \beta_k^1 F[\tilde{u}_h^{n+1}] + \beta_k^2 F[\tilde{u}_h^n], \quad u_{h,k}^0 = 0,$$

with coefficients

$$(5.13) \quad \begin{aligned} \gamma_k &= e^{-d_k h}, & \beta_k^1 &= c_k \frac{\gamma_k - (1 - d_k h)}{d_k^2 h}, & \beta_k^2 &= c_k \frac{1 - (1 + d_k h)\gamma_k}{d_k^2 h}, \\ \beta &= \sum_{k=1}^m (\beta_k^1 + \beta_k^2) + c_\infty = \sum_{k=1}^m \frac{c_k}{d_k} (1 - \gamma_k) + c_\infty. \end{aligned}$$

Then, \tilde{u}_h^n approximates $\tilde{u}(t)$, provided the discretization error of order $h^{1+\alpha}$:

$$\epsilon_h^n = \|\tilde{u}(t^n) - \tilde{u}_h^n\|_{\mathcal{H}} \leq \mathcal{O}(h^{1+\alpha}) \cdot e^{2C_F[(t^n)^\alpha + \varepsilon_{ra}]},$$

where $\varepsilon_{ra} := \max_{s \in [\frac{1}{T}, \frac{1}{h}]} |\hat{K}(s) - \hat{\tilde{K}}(s)|$ stands for the rational approximation error.

Proof. From (3.3), the modes satisfy the recurrence relation

$$(5.14) \quad u_k(t^{n+1}) = u_k(t^n) e^{-d_k h} + c_k \int_{t^n}^{t^{n+1}} e^{-d_k(t-s)} F(s, \tilde{u}(s)) ds.$$

Let us consider the following quadrature rule for an arbitrary function $f(t)$ and scalar $\lambda \geq 0$:

$$\begin{aligned} \int_{t^n}^{t^{n+1}} e^{-\lambda(t-s)} f(s) ds &= a_1 \frac{f(t^{n+1}) + f(t^n)}{2} + a_2 \frac{f(t^{n+1}) - f(t^n)}{h} + \mathcal{O}(a_1 h^2) \\ &= \left(\frac{a_1}{2} + \frac{a_2}{h}\right) f(t^{n+1}) + \left(\frac{a_1}{2} - \frac{a_2}{h}\right) f(t^n) + \mathcal{O}(a_1 h^2) \end{aligned}$$

with coefficients given as

$$a_1 = a_1(\lambda) = \int_0^h e^{-\lambda s} ds \leq \frac{2h}{1+\lambda h}, \quad a_2 = a_2(\lambda) = \int_0^h e^{-\lambda s} \left(\frac{h}{2} - s\right) ds$$

Applying the above quadrature rule to (5.14), given $\beta_k^1 := c_k \left(\frac{a_1(d_k)}{2} + \frac{a_2(d_k)}{h}\right)$ and $\beta_k^2 = c_k \left(\frac{a_1(d_k)}{2} - \frac{a_2(d_k)}{h}\right)$, we obtain

$$(5.15) \quad u_k(t^{n+1}) = \gamma_k u_k(t^n) + \beta_k^1 F[\tilde{u}](t^{n+1}) + \beta_k^2 F[\tilde{u}](t^n) + \mathcal{O}(c_k a_1(d_k) h^2).$$

Note that $0 \leq a_1(d_k) \leq \frac{2h}{1+d_k h}$ and thus $0 \leq \sum_{k=1}^m c_k a_1(d_k) \leq 2h^\alpha - c_\infty \leq 2h^\alpha$. Summing up the modes, u_0 and u_∞ , we obtain

$$\tilde{u}(t^{n+1}) - \beta^1 F[\tilde{u}](t^{n+1}) = \beta^2 F[\tilde{u}](t^n) + u_0 + \sum_{k=1}^m \gamma_k u_k(t^n) + \mathcal{O}(h^{2+\alpha}),$$

where

$$(5.16) \quad \beta^1 := \sum_{k=0}^m \beta_k^1 + c_\infty \quad \text{and} \quad \beta^2 := \sum_{k=0}^m \beta_k^2.$$

Note that $\beta_k^1 + \beta_k^2 \leq 2\frac{c_k h}{1+d_k h}$ and thus $\beta^1 + \beta^2 = \mathcal{O}(h^\alpha)$. Then, using Taylor expansion of $F_+[\tilde{u}](t^{n+1})$ at the point t^n and respectively $F_-[\tilde{u}](t^n)$ at the point t^{n+1} , we write

$$(5.17) \quad \tilde{u}(t^{n+1}) - \beta F_-[\tilde{u}](t^{n+1}) = \beta F_+[\tilde{u}](t^n) + u_0 + \sum_{k=1}^m \gamma_k u_k(t^n) + \mathcal{O}(h^{1+\alpha}).$$

We subtract (5.11) and (5.12) from (5.17) and (5.15), respectively, to obtain

$$(5.18) \quad \epsilon_h^{n+1} \leq \beta C_F \epsilon_h^n + \sum_{k=1}^m \gamma_k \epsilon_{h,k}^n + \mathcal{O}(h^{1+\alpha}),$$

and

$$(5.19) \quad \epsilon_{h,k}^{n+1} \leq \gamma_k \epsilon_{h,k}^n + C_F (\beta_k^1 \epsilon_h^{n+1} + \beta_k^2 \epsilon_h^n) + \mathcal{O}\left(\frac{c_k h^3}{1 + d_k h}\right), \quad \epsilon_{h,k}^0 = 0.$$

where we used continuity of F and monotonicity of F_- as in (5.8). Recursive substitution in (5.19), yields to

$$\epsilon_{h,k}^n \leq C_F \sum_{j=1}^n (\beta_k^1 + \beta_k^2) \gamma_k^{n-j} \epsilon_h^j + \mathcal{O}\left(\frac{c_k h^2}{1 + d_k h}\right).$$

Substituting this to (5.18), we thus write the estimation

$$\epsilon_h^{n+1} \leq C_F \left(\beta \epsilon_h^n + \sum_{k=1}^m \sum_{j=1}^n (\beta_k^1 + \beta_k^2) \gamma_k^{n+1-j} \epsilon_h^j \right) + \mathcal{O}(h^{1+\alpha}), \quad \epsilon_h^0 = 0.$$

Hence, by the discrete Grönwall inequality, we finally obtain

$$\epsilon_h^n \leq \mathcal{O}(h^{1+\alpha}) \cdot e^{C_F [\sum_{k=1}^m \sum_{j=0}^{n-1} (\beta_k^1 + \beta_k^2) \gamma_k^j + c_\infty]} \leq \mathcal{O}(h^{1+\alpha}) \cdot e^{2 C_F [(t^n)^\alpha + \varepsilon_{ra}]},$$

using the following bound for the exponent:

$$\sum_{j=0}^{n-1} (\beta_k^1 + \beta_k^2) \gamma_k^j = \frac{c_k}{d_k} (1 - \gamma_k) \frac{1 - \gamma_k^n}{1 - \gamma_k} = c_k \int_0^{t^n} e^{-d_k t} dt \leq 2 \frac{c_k t^n}{1 + d_k t^n}.$$

□

Remark 5.7. Note that the schemes presented in Lemmas 5.4 and 5.6 are of the implicit-explicit (IMEX) type. In particular, the explicit modal system defines the order of the scheme, while the implicit part, summing up the modes to the solution, guarantees stability via splitting of the operator.

Remark 5.8. In contrast to the common strategy, when the fractional integral is split into the local and the history integrals (see, e.g., [60, 3, 62]), we did not discretize the local integral explicitly in the construction of our schemes. Instead, the local term is obtained as linear combination of the modes (including the "infinity" mode u_∞ which does not however enter to the history part). Moreover, let us remark that the coefficients β^1 and β^2 in (5.16) approximate the 2nd order fractional Adams–Moulton coefficients [60], $\beta_{AM}^1 = h^\alpha / \Gamma(\alpha + 2)$ and $\beta_{AM}^2 = \alpha h^\alpha / \Gamma(\alpha + 2)$, respectively. The values of the coefficients for $\alpha = 0.1$ and $\alpha = 0.9$ are compared in Figure 3. Thus, using Adams–Moulton type discretization for the modal equations, the rational approximation approach can automatically reconstruct the fractional Adams–Moulton coefficients, naturally leading to the local integration term arising in fractional linear multi-step methods.

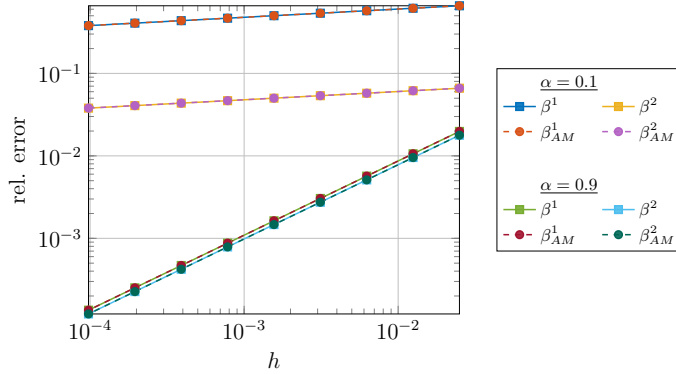


Fig. 3: Comparison of the coefficients β^1 and β^2 in (5.13) for the modified Crank-Nicolson scheme (Lemma 5.6) with the 2nd order fractional Adams-Moulton coefficients $\beta_{AM}^1 = h^\alpha/\Gamma(\alpha+2)$ and $\beta_{AM}^2 = \alpha h^\alpha/\Gamma(\alpha+2)$, respectively.

6. Numerical examples. In this section, we illustrate the proposed scheme in application to the two following examples. We first consider a simple linear case, more precisely, the one-dimensional fractional heat equation, where the analytical solution is known and given by a Mittag-Leffler function, so that we can study the accuracy and convergence rate. Then, the scheme is applied to the more complex non-linear Cahn-Hilliard equation and compared to a classical fractional time-stepping scheme. Both problems are discretized in space with Finite Elements using the FEniCS package [1].

6.1. Fractional heat equation. Let us consider one-dimensional fractional heat equation with homogeneous Dirichlet boundary conditions:

$$\begin{aligned} \partial_t^\alpha u(t, x) - \partial_x^2 u(t, x) &= 0, \quad t > 0, \quad x \in (0, 1), \\ u(0, x) &= \sin(\pi x), \\ u(t, 0) &= u(t, 1) = 0. \end{aligned}$$

Its analytical solution is given by $u(t, x) = E_{\alpha,1}[-\pi^2 t^\alpha] \sin(\pi x)$, see, e.g., [35], where $E_{\alpha,\beta}[x]$ is the Mittag-Leffler function (4.3). Note that in this example, we have $F[v] = F_-[v] = \partial_x^2 v$, i.e. $F_+[v] \equiv 0$. And thus, the scheme in Lemma 5.4 coincides with the implicit Euler scheme in Proposition 5.1 ($\theta = 1$).

The solution of a FDE usually has a weak singularity at the initial time and thus pollutes the error at the beginning of the time interval. Thus, the optimal convergence rate can then not be observed globally. Therefore, the error in the origin has to be treated in a special way, see, e.g., [41, 62]. Here we just ignore this effect and consider the error on the shortened interval $[T/3, T]$, where the effect of the initial singularity has been faded out. So, we are going to study the relative error $\mathcal{E}_r := \|u - \tilde{u}_h\|_2 / \|u - u_0\|_2$, where the norm is defined via ℓ_2 -norm in time on the shortened interval $[T/3, T]$ and L^2 -norm in space (using FE). We use 1000 P_1 -elements for the space discretization and the AAA-tolerance 10^{-13} with 100 support points for the rational approximation.

We start with a comparison of the Crank-Nicolson scheme with its stable modification (Lemma 5.6). The corresponding solutions (norms) with the time step size $h = 10^{-3}$ for the cases $\alpha = 0.1, 0.3, 0.5$ are shown on Figure 4. There we observe

oscillations for the CN scheme (left) but not for the modified one (right). Moreover, the oscillations become stronger when α decreases.

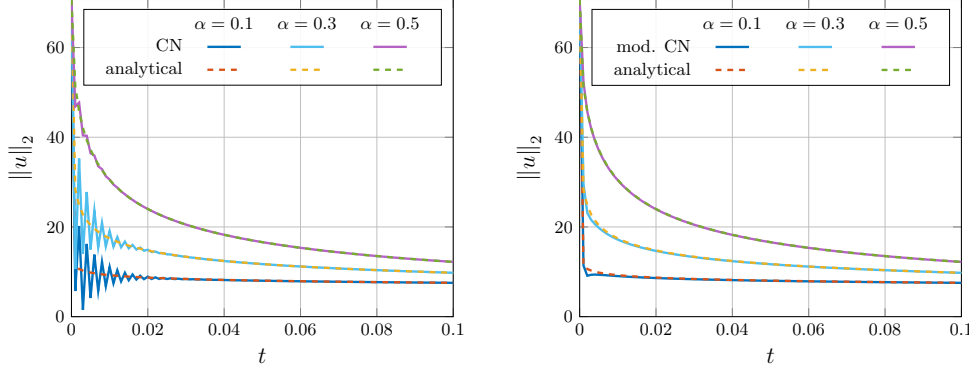


Fig. 4: Illustration of instability effects of the Crank-Nicolson scheme (left) for $\alpha = 0.1, 0.3, 0.5$ with $h = 10^{-3}$. The effect is stronger for smaller α . However, there is no oscillatory effect in case of the modified scheme (5.11)-(5.12) (right).

Then, we study the convergence rate of the relative error \mathcal{E}_r with respect to the time step size h for the Implicit Euler scheme (5.4)-(5.5) and the modified Crank-Nicolson scheme (5.11)-(5.12). The results for $\alpha = 1, 0.8, 0.5, 0.3, 0.1, 0.03, 0.01$ are plotted in Figure 5 and confirm the theoretical error bounds suggested in Lemmas 5.4 and 5.6, respectively. In particular, for the first scheme, we clearly observe linear convergence rate for all α , while the second scheme presents convergence of order $h^{1+\alpha}$.

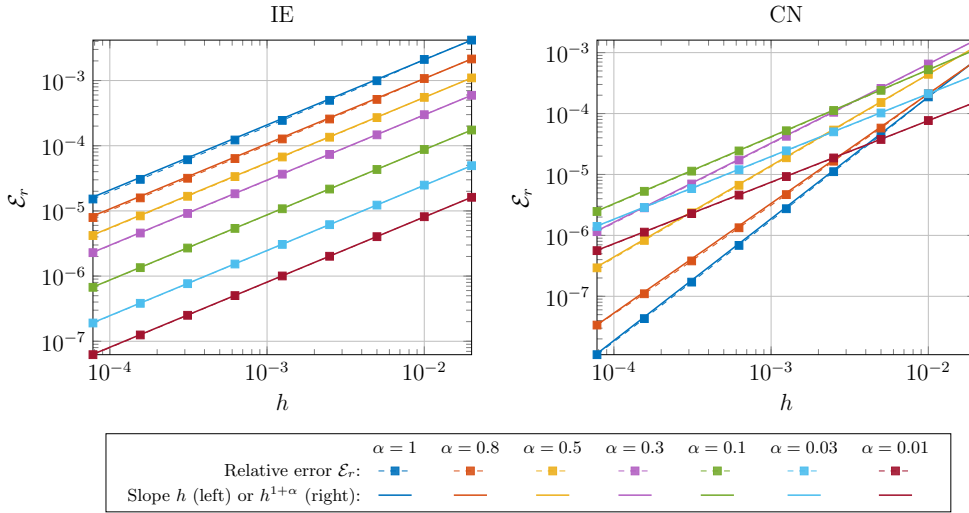


Fig. 5: Convergence rate of the Implicit Euler scheme (5.4)-(5.5) (left) and the modified Crank-Nicolson scheme (5.11)-(5.12) (right).

6.2. Fractional Cahn-Hilliard equation. Let $\Omega = (0, 1)^2$ be a unit square domain and $\mathcal{B} = L^2([0, T]; \mathcal{H})$, where $\mathcal{H} = H^1(\Omega) \times H^1(\Omega)$. Moreover, let $\langle \cdot, \cdot \rangle$ and $\|\cdot\|$ denote the scalar product and the norm in $L^2(\Omega)$, respectively. Then, we formulate the following non-linear Cahn-Hilliard problem: find $(u, \mu) \in \mathcal{B}$ satisfying for all $(v, w) \in \mathcal{H}$ and all $t \in (0, T]$,

$$(6.1) \quad \begin{aligned} \langle \partial_t^\alpha u, v \rangle &= -\langle M \nabla \mu, \nabla v \rangle, \\ \langle \mu, w \rangle &= \langle \psi(u), w \rangle + \varepsilon^2 \langle \nabla u, \nabla w \rangle, \end{aligned}$$

provided homogeneous Neumann boundary conditions, the initial state $u(0) = u_0$, the constant mobility M and the surface parameter ε . The non-linear function $\psi(u)$ is defined as derivative of the potential $\Phi(u) = \frac{1}{4}(u^2 - 1)^2$:

$$\psi(u) = \Phi'(u) = u^3 - u.$$

The Ginzburg–Landau free energy of the system is defined as

$$E(u) = \int_{\Omega} \left[\Phi(u) + \frac{\varepsilon^2}{2} |\nabla u|^2 \right] d\Omega.$$

Note that the function $\psi(u)$ is Lipschitz continuous on the interval $[-1, 1]$, i.e., between zeros of the potential $\Phi(u)$. Therefore, if the initial conditions are contained in the interval, the problem (6.1) satisfies the conditions of Theorem 4.3.

Due to the "double-well" structure of the potential, presenting both convex and concave parts, stability of time-schemes for Cahn-Hilliard equation is a sophisticated question and is a subject of numerous works. The fully implicit time-schemes are only conditionally stable [25]. Unconditionally stable schemes include so-called gradient stability, providing monotone decay of the discretized Ginzburg–Landau energy, e.g., splitting to implicit convex and explicit concave parts [27, 57] or others [24, 30]. The situation becomes more complicated in the case of fractional derivative, since even for the analytical solution, the associated Ginzburg–Landau energy is not proved to be monotone [54]. Note that the schemes presented in Lemmas 5.4 and 5.6 naturally allow splitting techniques, ensuring stability. Splitting the potential into convex and concave parts, we consider $\psi(u) = \psi_+(u) + \psi_-(u)$, where the functions $\psi_+(u)$ and $\psi_-(u)$ are monotonously increasing and decreasing in $[-1, 1]$, respectively. Note that such splitting is not unique. Let us use the following splitting scheme, proposed in [28]:

$$(6.2) \quad \psi_+(u) = 2u, \quad \psi_-(u) = u^3 - 3u.$$

Let \mathcal{H} be an appropriate finite elements space. Implementing the modified Crank-Nicolson scheme (5.11)-(5.13) for discretization of the problem (6.1), we compute at each time step n the discrete solution pair $(u_h^{n+1}, \mu_h^{n+1}) \in \mathcal{H}$ satisfying

$$(6.3) \quad \begin{aligned} \langle u_h^{n+1} - H^n, v \rangle &= -\beta \langle M \nabla \tilde{\mu}_h^{n+1}, \nabla v \rangle, \\ \langle \tilde{\mu}_h^{n+1}, w \rangle &= \langle \psi_+(u_h^{n+1}) + \psi_-(u_h^n), w \rangle + \varepsilon^2 \langle \nabla u_h^{n+1}, \nabla w \rangle, \end{aligned}$$

for all $(v, w) \in \mathcal{H}$, with the history term defined as $H^n = u_0 + \sum_{k=1}^n \gamma_k u_{h,k}^n$, where the modes u_k^n , $k = 1, \dots, m$, are updated as follows:

$$(6.4) \quad \begin{aligned} \langle u_{h,k}^{n+1}, v \rangle &= \gamma_k \langle u_{h,k}^n, v \rangle - \langle M \nabla [\beta_k^1 \mu^{n+1} + \beta_k^2 \mu^n], \nabla v \rangle, \quad u_{h,k}^0 = 0, \\ \langle \mu_h^{n+1}, w \rangle &= \langle \psi(u_h^{n+1}), w \rangle + \varepsilon^2 \langle \nabla u_h^{n+1}, \nabla w \rangle, \end{aligned}$$

with the coefficients β , β_k^1 , β_k^2 and γ_k given in (5.13). Remark that a linear choice of the increasing part in (6.2) leads to a linear implicit part in the time-scheme. That is, though the problem (6.1) is non-linear, the numerical solution of (6.3) requires only a linear solver at each time step.

For our simulation, we fix the constant mobility $M = 0.05$, the surface parameter $\varepsilon = 0.03$ and the final time $T = 4$. For discretization in space, we use (Q_1, Q_1) elements on a 64×64 quadrilateral mesh. For the rational approximation, we use the AAA-tolerance 10^{-12} with 100 support points. The initial state is

$$u_0(\mathbf{x}) = \sum_{i=1}^4 \tanh \frac{r - |\mathbf{x} - \mathbf{x}_i|}{\sqrt{2}\varepsilon} + 3, \quad \mathbf{x} \in \Omega,$$

with $\mathbf{x}_1 = (0.3, 0.3)$, $\mathbf{x}_2 = (0.3, 0.7)$, $\mathbf{x}_3 = (0.7, 0.7)$, $\mathbf{x}_4 = (0.7, 0.3)$ and $r = 0.15$, which corresponds to four bubbles of radius r centered at \mathbf{x}_i . Due to the surface tension, the bubbles tend to coalesce in time [38]. However, the process proceeds with different speed for different values of the fractional order α . In particular, for a small α , the coalescence accelerates in the beginning but then slows down with respect to larger values of α . This effect can be observed in Figure 6, where different states (computed with $h = 2^{-14}$) are shown for $\alpha = 0.1, 0.3, 0.5, 0.9$ at time $t = 0, 0.4, 3.2, 4$. Such behavior is also observed for the evolution of the corresponding Ginzburg–Landau energies, which is depicted in Figure 7 on the left. These solutions are taken as reference for the convergence study of the relative error $\mathcal{E}_r := \|u - u_h\|_2 / \|u - u_0\|_2$, where the norm is again defined via ℓ_2 -norm in time on the shortened interval $[T/3, T]$ and L^2 -norm in \mathcal{H} . In Figure 7 on the right, there are plotted the convergence rates of the error with respect to the time step size h for the same values of α . We can observe that the error convergence respects the theoretical bounds.

7. Conclusion. In this work, we proposed a new numerical method for solving fractional in time differential equation. The method is based on the approximation of the Laplace spectrum of the fractional convolution kernel with a rational function, more precisely, a multi-pole series with an additional constant term. To this end, we used the barycentric rational interpolation with the adaptive Antoulas–Anderson (AAA) algorithm. This leads to the approximation of the kernel itself with a sum-of-exponentials with an additional singular term. Thus, the solution of the FODE is represented as a sum of a small number of modes which solve a system of ODEs and can be updated in parallel. Since the number of modes is fixed and defined only by the fractional kernel, the computational complexity and the memory load is constant for each time step. We proposed the associated variants of the implicit Euler and Crank–Nicolson numerical schemes with convergence orders $\mathcal{O}(h)$ and $\mathcal{O}(h^{1+\alpha})$, respectively. The accuracy of the schemes is illustrated using a linear problem with known analytical solution. The method has been also applied to a non-linear fractional Cahn–Hilliard problem in 2D.

REFERENCES

- [1] M. S. Alnæs, J. Blechta, J. Hake, A. Johansson, B. Kehlet, A. Logg, C. Richardson, J. Ring, M. E. Rognes, and G. N. Wells. The fenics project version 1.5. *Archive of Numerical Software*, 3(100), 2015.
- [2] D. Baffet. A gauss–jacobi kernel compression scheme for fractional differential equations. *Journal of Scientific Computing*, 79(1):227–248, 2019.
- [3] D. Baffet and J. S. Hesthaven. A kernel compression scheme for fractional differential equations. *SIAM Journal on Numerical Analysis*, 55(2):496–520, 2017.

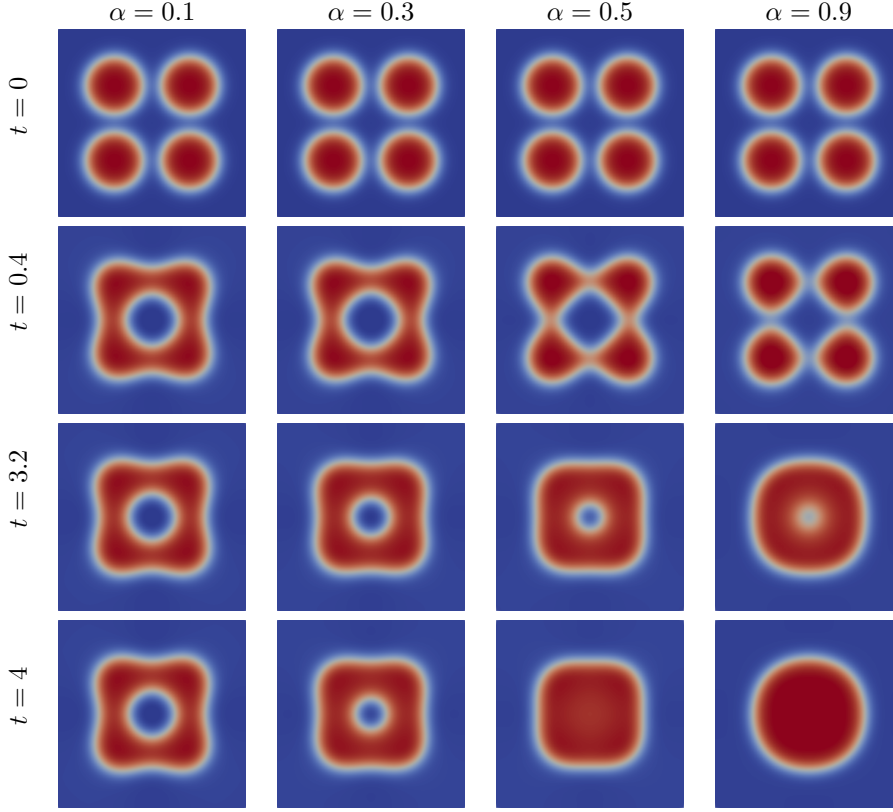


Fig. 6: Fractional non-linear Cahn-Hilliard equation with $\alpha = 0.1, 0.3, 0.5, 0.9$. Four bubbles coalesce with different speed: for smaller α , the coalescence accelerates in the beginning but then slows down with respect to larger values of α .

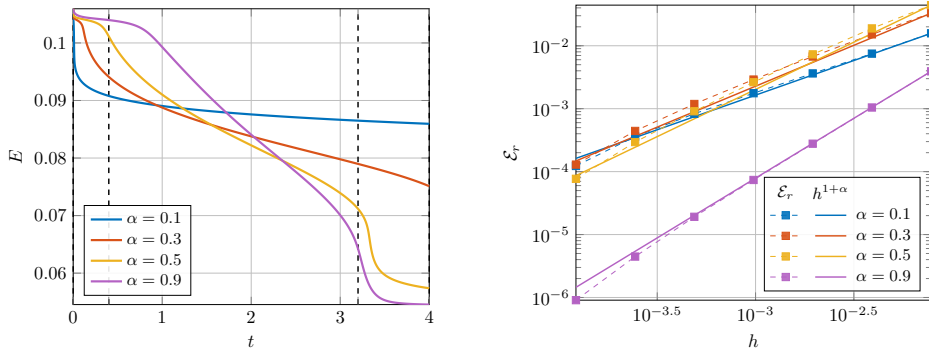


Fig. 7: Fractional non-linear Cahn-Hilliard equation with $\alpha = 0.1, 0.3, 0.5, 0.9$. **Left:** Evolution in time of the Ginzburg–Landau energy. **Right:** Convergence rate for the rational approximation based scheme (6.3)–(6.4).

- [4] E. G. Bajlekova et al. *Fractional evolution equations in Banach spaces*. Citeseer, 2001.
- [5] G. A. Baker, G. A. Baker Jr, G. Baker, P. Graves-Morris, and S. S. Baker. *Pade Approximants: Encyclopedia of Mathematics and Its Applications, Vol. 59 George A. Baker, Jr., Peter Graves-Morris*, volume 59. Cambridge University Press, 1996.
- [6] D. Baleanu, K. Diethelm, E. Scalas, and J. J. Trujillo. *Fractional calculus: models and numerical methods*, volume 3. World Scientific, 2012.
- [7] L. Banjai and M. López-Fernández. Efficient high order algorithms for fractional integrals and fractional differential equations. *Numerische Mathematik*, 141(2):289–317, 2019.
- [8] L. Banjai, J. M. Melenk, R. H. Nochetto, E. Otarola, A. J. Salgado, and C. Schwab. Tensor fem for spectral fractional diffusion. *Foundations of Computational Mathematics*, 19(4):901–962, 2019.
- [9] J.-P. Berrut, R. Baltensperger, and H. D. Mittelmann. Recent developments in barycentric rational interpolation. In *Trends and applications in constructive approximation*, pages 27–51. Springer, 2005.
- [10] G. Beylkin and L. Monzón. On approximation of functions by exponential sums. *Applied and Computational Harmonic Analysis*, 19(1):17–48, 2005.
- [11] A. Bonito and J. Pasciak. Numerical approximation of fractional powers of elliptic operators. *Mathematics of Computation*, 84(295):2083–2110, 2015.
- [12] L. Caffarelli and L. Silvestre. An extension problem related to the fractional laplacian. *Communications in partial differential equations*, 32(8):1245–1260, 2007.
- [13] O. S. Celis and A. Cuyt. *Practical rational interpolation of exact and inexact data: theory and algorithms*. Universiteit Antwerpen, Faculteit Wetenschappen, Departement Wiskunde . . . , 2008.
- [14] W. Deng. Short memory principle and a predictor–corrector approach for fractional differential equations. *Journal of Computational and Applied Mathematics*, 206(1):174–188, 2007.
- [15] K. Diethelm. An investigation of some nonclassical methods for the numerical approximation of Caputo-type fractional derivatives. *Numerical Algorithms*, 47(4):361–390, 2008.
- [16] K. Diethelm. An investigation of some nonclassical methods for the numerical approximation of caputo-type fractional derivatives. *Numerical Algorithms*, 47(4):361–390, 2008.
- [17] K. Diethelm. *The analysis of fractional differential equations: An application-oriented exposition using differential operators of Caputo type*. Springer Science & Business Media, 2010.
- [18] K. Diethelm. An efficient parallel algorithm for the numerical solution of fractional differential equations. *Fractional Calculus and Applied Analysis*, 14(3):475–490, 2011.
- [19] K. Diethelm, J. M. Ford, N. J. Ford, and M. Weilbeer. Pitfalls in fast numerical solvers for fractional differential equations. *Journal of computational and applied mathematics*, 186(2):482–503, 2006.
- [20] K. Diethelm, N. J. Ford, and A. D. Freed. A predictor-corrector approach for the numerical solution of fractional differential equations. *Nonlinear Dynamics*, 29(1-4):3–22, 2002.
- [21] K. Diethelm, N. J. Ford, and A. D. Freed. Detailed error analysis for a fractional adams method. *Numerical algorithms*, 36(1):31–52, 2004.
- [22] K. Diethelm and A. D. Freed. An efficient algorithm for the evaluation of convolution integrals. *Computers & Mathematics with Applications*, 51(1):51–72, 2006.
- [23] K. Diethelm, R. Garrappa, and M. Stynes. Good (and not so good) practices in computational methods for fractional calculus. *Mathematics*, 8(3):324, 2020.
- [24] Q. Du and R. A. Nicolaides. Numerical analysis of a continuum model of phase transition. *SIAM Journal on Numerical Analysis*, 28(5):1310–1322, 1991.
- [25] C. M. Elliott. The cahn-hilliard model for the kinetics of phase separation. In *Mathematical models for phase change problems*, pages 35–73. Springer, 1989.
- [26] C. L. Epstein and J. Schotland. The bad truth about laplace’s transform. *SIAM review*, 50(3):504–520, 2008.
- [27] D. J. Eyre. Unconditionally gradient stable time marching the cahn-hilliard equation. In *Materials Research Society Symposium Proceedings*, volume 529, pages 39–46. Materials Research Society, 1998.
- [28] D. J. Eyre. An unconditionally stable one-step scheme for gradient systems. *Unpublished article*, pages 1–15, 1998.
- [29] N. J. Ford and A. C. Simpson. The numerical solution of fractional differential equations: speed versus accuracy. *Numerical Algorithms*, 26(4):333–346, 2001.
- [30] H. Gomez and T. J. Hughes. Provably unconditionally stable, second-order time-accurate, mixed variational methods for phase-field models. *Journal of Computational Physics*, 230(13):5310–5327, 2011.
- [31] S. Harizanov and S. Margenov. *Positive approximations of the inverse of fractional powers of*

- SPD M-matrices*, pages 147–163. Springer, 2018.
- [32] S. Jiang, J. Zhang, Q. Zhang, and Z. Zhang. Fast evaluation of the caputo fractional derivative and its applications to fractional diffusion equations. *Communications in Computational Physics*, 21(3):650–678, 2017.
 - [33] B. Jin, R. Lazarov, and Z. Zhou. An analysis of the l1 scheme for the subdiffusion equation with nonsmooth data. *IMA Journal of Numerical Analysis*, 36(1):197–221, 2016.
 - [34] E. Jones, T. Oliphant, P. Peterson, et al. SciPy: Open source scientific tools for Python, 2001–.
 - [35] L. Kexue and P. Jigen. Laplace transform and fractional differential equations. *Applied Mathematics Letters*, 24(12):2019–2023, 2011.
 - [36] A. A. Kilbas, H. M. Srivastava, and J. J. Trujillo. *Theory and applications of fractional differential equations*, volume 204. elsevier, 2006.
 - [37] J.-R. Li. A Fast Time Stepping Method for Evaluating Fractional Integrals. *SIAM Journal on Scientific Computing*, 31(6):4696–4714, 2010.
 - [38] H. Liu, A. Cheng, H. Wang, and J. Zhao. Time-fractional allen–cahn and cahn–hilliard phase-field models and their numerical investigation. *Computers & Mathematics with Applications*, 76(8):1876–1892, 2018.
 - [39] M. López-Fernández, C. Lubich, and A. Schädle. Adaptive, fast, and oblivious convolution in evolution equations with memory. *SIAM Journal on Scientific Computing*, 30(2):1015–1037, 2008.
 - [40] C. Lubich. On the stability of linear multistep methods for volterra convolution equations. *IMA Journal of Numerical Analysis*, 3(4):439–465, 1983.
 - [41] C. Lubich. Discretized fractional calculus. *SIAM Journal on Mathematical Analysis*, 17(3):704–719, 1986.
 - [42] C. Lubich. Convolution quadrature and discretized operational calculus. i. *Numerische Mathematik*, 52(2):129–145, 1988.
 - [43] C. Lubich and A. Schädle. Fast convolution for nonreflecting boundary conditions. *SIAM Journal on Scientific Computing*, 24(1):161–182, 2002.
 - [44] F. Mainardi. *Fractional calculus and waves in linear viscoelasticity: an introduction to mathematical models*. World Scientific, 2010.
 - [45] W. McLean. Exponential sum approximations for $t^{-\beta}$. In *Contemporary Computational Mathematics-A Celebration of the 80th Birthday of Ian Sloan*, pages 911–930. Springer, 2018.
 - [46] W. McLean, I. H. Sloan, and V. Thomée. Time discretization via laplace transformation of an integro-differential equation of parabolic type. *Numerische Mathematik*, 102(3):497–522, 2006.
 - [47] K. S. Miller and B. Ross. *An introduction to the fractional calculus and fractional differential equations*. Wiley, 1993.
 - [48] Y. Nakatsukasa, O. Sète, and L. N. Trefethen. The aaa algorithm for rational approximation. *SIAM Journal on Scientific Computing*, 40(3):A1494–A1522, 2018.
 - [49] K. Oldham and J. Spanier. *The fractional calculus theory and applications of differentiation and integration to arbitrary order*. Elsevier, 1974.
 - [50] I. Podlubny. *Fractional differential equations: an introduction to fractional derivatives, fractional differential equations, to methods of their solution and some of their applications*. Elsevier, 1998.
 - [51] S. G. Samko, A. A. Kilbas, O. I. Marichev, et al. *Fractional integrals and derivatives*, volume 1. Gordon and Breach Science Publishers, Yverdon Yverdon-les-Bains, Switzerland, 1993.
 - [52] A. Schädle, M. López-Fernández, and C. Lubich. Fast and oblivious convolution quadrature. *SIAM Journal on Scientific Computing*, 28(2):421–438, 2006.
 - [53] H. R. Stahl. Best uniform rational approximation of x^α on $[0, 1]$. *Acta mathematica*, 190(2):241–306, 2003.
 - [54] T. Tang, H. Yu, and T. Zhou. On energy dissipation theory and numerical stability for time-fractional phase-field equations. *SIAM Journal on Scientific Computing*, 41(6):A3757–A3778, 2019.
 - [55] L. N. Trefethen. *Approximation theory and approximation practice*, volume 164. Siam, 2019.
 - [56] P. N. Vabishchevich. Numerically solving an equation for fractional powers of elliptic operators. *Journal of Computational Physics*, 282:289–302, 2015.
 - [57] X. Wu, G. Van Zwielen, and K. Van der Zee. Stabilized second-order convex splitting schemes for cahn–hilliard models with application to diffuse-interface tumor-growth models. *International journal for numerical methods in biomedical engineering*, 30(2):180–203, 2014.
 - [58] H. Ye, J. Gao, and Y. Ding. A generalized gronwall inequality and its application to a fractional differential equation. *Journal of Mathematical Analysis and Applications*, 328(2):1075–1081, 2007.

- [59] L. Yuan and O. P. Agrawal. A numerical scheme for dynamic systems containing fractional derivatives. *Journal of Vibration and Acoustics, Transactions of the ASME*, 124(2):321–324, 2002.
- [60] M. Zayernouri and A. Matzavinos. Fractional adams–bashforth/moulton methods: an application to the fractional keller–segel chemotaxis system. *Journal of Computational Physics*, 317:1–14, 2016.
- [61] F. Zeng, I. Turner, and K. Burrage. A stable fast time-stepping method for fractional integral and derivative operators. *Journal of Scientific Computing*, 77(1):283–307, 2018.
- [62] Y. Zhou, J. L. Suzuki, C. Zhang, and M. Zayernouri. Fast imex time integration of nonlinear stiff fractional differential equations. *arXiv preprint arXiv:1909.04132*, 2019.